
Selection of Aptamers for Sensing Caffeine and Discrimination of Its Three Single Demethylated Analogs

Po-Jung Jimmy Huang and Juewen Liu*

Department of Chemistry, Waterloo Institute for Nanotechnology University of Waterloo
200 University Avenue West, Waterloo, Ontario, N2L 3G1, Canada
E-mail: liujw@uwaterloo.ca

Abstract: With the growing consumption of caffeine-containing beverages, detection of caffeine has become an important biomedical, bioanalytical and environmental topic. We herein isolated four high-quality aptamers for caffeine with dissociation constants ranging from 2.2 to 14.6 μM as characterized using isothermal titration calorimetry. Different binding patterns were obtained for the three single demethylated analogs: theobromine, theophylline and paraxanthine, highlighting the effect of molecular symmetry of the arrangement of the three methyl groups in caffeine. A structure-switching fluorescent sensor was designed showing a detection limit of 1.2 μM caffeine, which reflected the labeled caffeine concentration within 6.1% difference for eight commercial beverages. In 20% human serum, a detection limit of 4.0 μM caffeine was achieved. With the four aptamer sensors forming an array, caffeine and the three analogs were well separated from nine other closely related molecules.

Introduction

Caffeine is the main biologically active component of tea, coffee and many other beverages. Aside from its stimulating effects to the neural system, caffeine also has roles in diabetes, cancer and heart rhythms problems.¹ The growing use of caffeine-containing drinks has made it an emergent environmental contaminant in water,² and caffeine was proposed as an indicator of domestic wastewater.³ Therefore, efforts have been made to develop analytical methods to detect caffeine. Aside from analytical instrumentation such as mass spectrometry coupled with HPLC,⁴ a few sensors including molecular fluorescent probes,⁵⁻⁹ immunoassays,¹⁰ and nanomaterials such as graphene oxide¹¹ and lanthanide containing materials and molecularly imprinted polymers¹² have been reported. Sensors are attractive since they allow cost-effective and on-site detection.

The chemical name of caffeine is 1,3,7-trimethylxanthine, and removing one of its three methyl groups would generate three analogs: theophylline, theobromine or paraxanthine. These single demethylated analogs also play interesting biological functions. For example, theophylline can treat asthma and chronic obstructive pulmonary disease (COPD), although it has a narrow therapeutic index (5-20 mg/L),¹³ where higher concentrations would cause both acute and chronic adverse effects. Theobromine is predominately found in cacao and is used as a vasodilator, a diuretic, and a heart stimulant.¹⁴ In humans, paraxanthine is the main metabolite (~80%) of caffeine.¹⁵ Thus, discriminating caffeine along with these closely related analogs poses an interesting analytical challenge.

Aptamers are single-stranded nucleic acids with selective molecular binding properties.¹⁶⁻²⁰ Aptamers are particularly attractive for binding and detection of small molecules.^{21, 22} The majority of aptamers in riboswitches bind to small molecule metabolites or ions.²³ In the lab, aptamers were isolated using a combinatorial method called systematic evolution of ligands by exponential enrichment (SELEX).²⁴⁻³¹ An RNA aptamer for theophylline has been the most often cited example to highlight the selectivity of aptamers, and its affinity to caffeine is over 10000-fold weaker despite they differ by just a methyl group.³² This theophylline aptamer has been extensively used as a model system for designing various aptamer-based sensors and RNA switches both inside and outside cells.³³ To date, no aptamers were reported for binding caffeine. Given its analytical and biological importance, we herein performed an aptamer selection for caffeine. We discovered a group of four aptamers that can bind caffeine and the three analogs in different orientations governed by the distribution of the methyl groups, allowing not only the selective detection of caffeine but also a pattern recognition-based method for telling them apart.

Materials and Methods

Chemicals. The DNA samples used for the selection and sensing experiments were purchased from Integrated DNA Technologies (Coralville, IA, USA). The sequences are listed in Table S1 and S2. Thermo Scientific Pierce streptavidin agarose resin was purchased from Fisher Scientific (Ottawa, ON, Canada). Caffeine, theophylline, theobromine, adenosine, adenine, guanine, xanthine, uric acid, dextrose, dopamine, tryptophan, tyrosine, sodium chloride, magnesium chloride, sodium hydroxide, hydrochloric acid, human serum, and Amicon Ultra-0.5 centrifugal filter unit (3K and 10K) were purchased from Millipore-Sigma (Oakville, ON, Canada). 4-(2-Hydroxyethyl)piperazine-1-ethanesulfonic acid (HEPES) and its sodium salt form were from Biobasic Inc. (Markham, ON, Canada). Micro bio-spin chromatography columns and SsoFast EvaGreen supermix were from Bio-Rad. dNTP mix, Taq DNA polymerase with ThermoPol buffer, and the low molecular weight DNA ladder were from New England Biolabs (Ipswich, MA, USA). Sep-Pak C18 cartridges were purchased from Waters. All buffers and solutions were prepared with Milli-Q water.

SELEX. The library design (Table S1) and selection method (Figure S1) were based on Stojanovic's previous publications with a few modifications.^{34, 35} At the beginning of each round, the single-stranded library strand was first annealed with five times excess of biotinylated capture strand in the SELEX buffer (500 mM NaCl, 10 mM MgCl₂, and 50 mM HEPES at pH 7.5). The high salt buffer was intended for screening nonspecific electrostatic interactions. The annealed DNA was stored on an ice bath. Meanwhile, 250 μ L of streptavidin agarose resin was packed into a micro chromatography column and were washed five times with 500 μ L of the SELEX buffer to remove preservatives. The annealed DNA was then cycled through the column several time to achieve maximum binding by gravity flow (~3 min each time). The column was washed again twelve times with 500 μ L of SELEX buffer to remove non-bound or loosely bound library. Once the washing step was completed, 750 μ L of caffeine solution was introduced and the eluted DNA was collected by gravity flow. The collected DNA was further concentrated and purified with Milli-Q water using a 3k spin column. The final volume of the purified DNA was adjusted to 60 μ L. Here, we included a real-time PCR (RT-PCR) step using unmodified primers to monitor the selection progress and to determine the PCR cycles for library amplification. Then, the biotinylated reverse primer was used to obtain 1.8 mL of PCR products, which were further concentrated and purified down to 250 μ L with the strand separation buffer (250 mM NaCl, 50 mM HEPES at pH7.5) using a 10k spin column. Similar to the earlier steps, the purified PCR product was loaded onto a column and washed ten times with 500 μ L of strand separation buffer, and then 600 μ L of 0.2 M NaOH was added to the column and incubated for 15 min to elute the ssDNA library. The library was neutralized and then desalted with Milli-Q water using a 3k spin column. Finally, the purified library was dissolved in 55 μ L SELEX buffer. To maintain a consistent library concentration, the library was quantified using a NanoDrop 2000

spectrophotometer. Typically, 250 μL of 0.4 μM of the library was used for each round of selection except for the initial few rounds (See Figure S2A).

Sample preparation for DNA sequencing. The 12th, 15th, and 20th round libraries were subjected to PCR. These libraries were first subjected to a PCR with a combination of P5-501 and one of the P7-702, P7-703, or P7-704 sequencing primers (Table S2). These primers contained a unique index sequence to be used for the Illumina sequencing. The PCR products were purified with 2% agarose gel and extracted using a small DNA fragment extraction kit (IBI Scientific). The concentration of the eluted DNA was quantified using NanoDrop and the sequencing was submitted to McMaster University for analysis. Sequencing results were analyzed with Geneious Prime and MAFFT alignment software.

Isothermal titration calorimetry (ITC). MicroCal VP-ITC was used for the ITC experiments. DNA (9 μM , 2 mL) and target molecules (1 mM, 2 mL) were dissolved in the SELEX buffer and degassed for 10 min prior to measurement. A volume of 1.4 mL aptamer was loaded into the cell chamber and 300 μL target was loaded in the syringe. Except for an initial injection of 0.5 μL , 10 μL of target was titrated into the cell each time over 20 sec duration for a total of 20 injections at 25 °C. The spacing was set for 360 sec between each injection. The thermodynamic values were obtained by fitting the titration curves to a one-site binding model using the Origin software.

Sensing in buffer. The sensing experiments were performed in a 96-well plate using a SpectraMax M3 microplate reader. The stock of 2 μM sensor complex was formed by annealing the 200 pmol of FAM-labeled caffeine aptamer (Caff203-FAM) with 400 pmol of short quencher-labeled complementary strand (Caff203-Q) in 100 μL SELEX buffer. In a typical experiment, 100 μL sensor sample with 20 nM aptamer strand was used. The background fluorescence of the sensor was monitored for 5 min before 2 μL of caffeine or other molecules was added. The signaling kinetics were continuously monitored for 25 min ($E_x = 485 \text{ nm}$; $E_m = 520 \text{ nm}$). The experiments were run in triplicate and error bars indicate the standard deviations.

Real sample detection. Various type of beverages and caffeine pills were purchased from a local pharmacy. The caffeine pills (200 mg per tablet) were first dissolved in 200 mL Milli-Q water and filtered with a 0.2 μm cellulose acetate membrane to make a 1 mg/mL stock solution. The other beverages were used directly. For detection, 2 μL of the sample was directly added to 100 μL of 20 nM sensor. The same protocol described above was followed and the final fluorescence signal after 30 min was used for calculating the caffeine concentration based on a standard curve. For sensing in serum, human serum was diluted to 20% with the SELEX buffer, and the other steps were the same as detection in buffer except that the detection was performed using a Tecan Spark microplate reader. Since serum increased the

background fluorescence, the data were plotted using $(F-F_0)/F_0$ where F_0 is the fluorescence before adding caffeine and F is the fluorescence after adding caffeine.

Discriminant analysis. The responses of the four caffeine sensors after 20 min incubation were obtained for a total of 13 purine analogs and other small molecules (20 μ M). For each sensor and each compound, eight sets of replicates were collected using the same buffer and sensing conditions described above. These data were used to construct a training matrix to generate a 2D canonical plot using principal component analysis (PCA) from the Origin software.

Results and Discussion

SELEX for caffeine aptamers

The structures of caffeine and its three single demethylated analogs are shown in Figure 1A. Our main goal is to obtain a selective aptamer for caffeine. Our aptamer selection was based on the immobilization of the DNA library containing a 30-nt random region on streptavidin-coated beads via hybridization to a biotinylated complementary strand (Figure 1B).³⁴ A detailed selection scheme is presented in Figure S1 and the DNA sequences used are in Table S1 and S2. The DNA sequences that can bind caffeine and dissociate from the beads were collected and then amplified by PCR to seed the next round of selection.^{34, 36-38} The library was designed in such a way that the selected aptamers would have a hairpin structure. To track the selection progress, the eluted DNA was quantified using real-time PCR for each round, and the detailed incubation time and target concentration of each round are supplied in Figure S2.^{34, 39-46}

A total of 20 rounds of selection were performed, and counter selections against theophylline was introduced from round 13 to improve specificity for caffeine. At the end, the round 12, 15, and 20 libraries were subjected to deep sequencing yielding around 30,000 reads for each library. Only the round 20 library showed a good sequence alignment, yielding four main families (see Figure S3 for sequence alignment). The Mfold predicted secondary structures⁴⁷ of the aptamer regions from the four families are shown in Figure 1C-F. Among them, the sequence named Caff203 (Figure 1D) represents the largest family counting for 29% of the final library. The 18-nucleotide conserved sequence (the red region in Figure 1D and underlined in Figure S3) only appeared 22 times and 265 times in the round 12 and 15 libraries, respectively. From round 12 to 20, this sequence on average enriched by \sim 2.3-fold for each round of the selection.

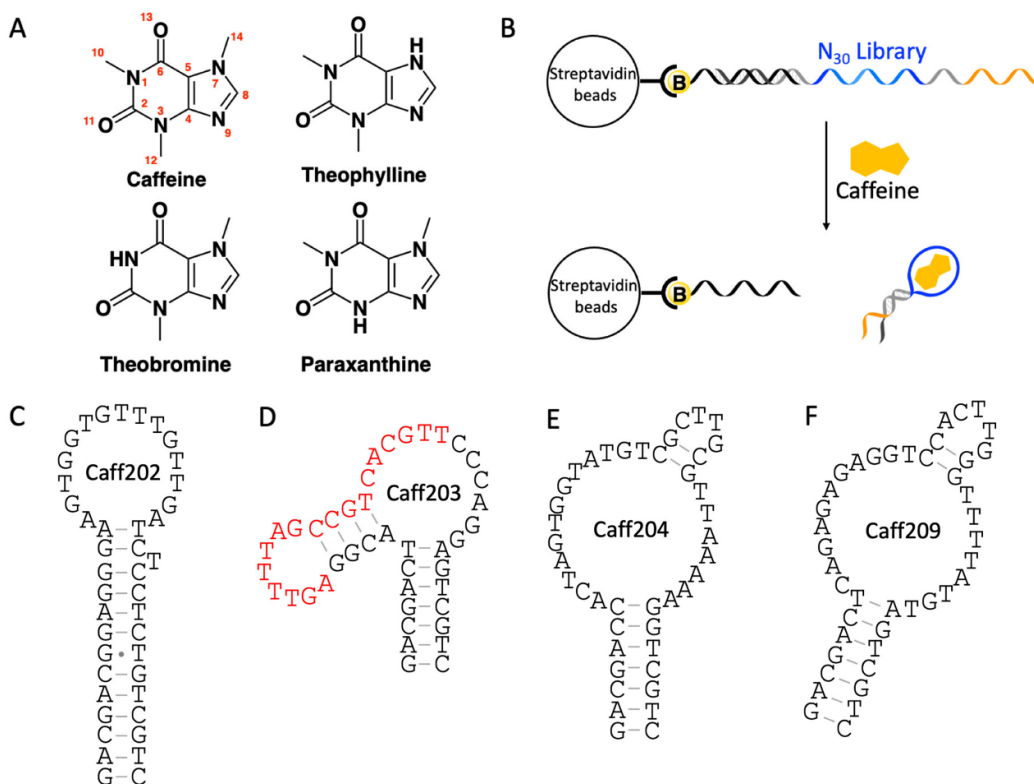


Figure 1. (A) Chemical structure of caffeine and its three single demethylated analogs. (B) The design of DNA library used in this study to obtain aptamers for caffeine. The library contained an N₃₀ random region flanked by two constant regions for immobilization (black region) and primer binding (orange region). The sequences eluted by caffeine were detached and collected for PCR amplification. (C-F) Secondary structure of the four caffeine binding aptamers predicted by Mfold.

Target symmetry directed binding

These sequences were individually tested using isothermal titration calorimetry (ITC), which is a label-free biophysical technique measuring the heat of binding.⁴⁸⁻⁵⁰ For each of the four aptamers, we titrated all of the four analogs separately. Their original ITC traces are shown in Figure 2, and the integrated heat and data fitting are shown in the insets. For all the titrations, the binding was exothermic as indicated by the downwards spikes. All the aptamers showed the strongest binding to caffeine, suggesting the SELEX was successful. For the three analogs, we noticed different binding patterns. Caff202 had a K_d of 14.6 μM for caffeine, no noticeable binding to theophylline or theobromine, and a small heat release with paraxanthine (K_d 36.4 μM). We reason that its binding geometry to caffeine might overlap with its binding to paraxanthine. Caff203 showed the strongest affinity to caffeine among these aptamers with a K_d of 2.2

μM . In addition, it also had a strong binding to theobromine ($K_d = 9.9 \mu\text{M}$). Based on its binding to theobromine, the N10 methyl group is not critical for caffeine binding. A few other analogs such as adenine, xanthine and uric acid showed no binding either (Figure S4). In the theophylline RNA aptamer, the N7 position in theophylline forms a critical hydrogen bond with its aptamer, and that's why it has excellent discrimination against caffeine and theobromine, both of which have a methyl group capping the N7 position.^{13, 51}

In these ITC experiments, we used an aptamer concentration of $9 \mu\text{M}$, and thus the c -value (defined as $[\text{aptamer}]/K_d$ for 1:1 binding) of those with a K_d larger than $9 \mu\text{M}$ would be smaller than one. It was proposed that the c -value needs to be greater than one for accurate fitting.⁵² One way to increase the c -value is to increase the aptamer concentration. However, when the aptamer concentration is too high (e.g., increased from 10 to $20 \mu\text{M}$ in one case), inter-aptamer interactions can also affect aptamer/target binding, leading to increased K_d .⁵⁰ In addition, Turnbull and Daranas pointed out that accurate results can still be obtained even when c -value is lower than one as long as binding saturation was achieved.⁵³ Therefore, we collected the data all under the same condition to have a fair comparison, and note that the high K_d values (e.g., $>30 \mu\text{M}$) from titrations with a small heat might be less accurate.

To confirm specific binding, mutations were made at two locations within the conserved region of Caff203. We mutated a fraction of the two loops by shuffling its bases (Figure S5A, Mutant-1 and Mutant-2), and both mutants completely lost binding (Figure S5B and S5C). Therefore, both loop regions are critical for binding of caffeine. This experiment indicated the above observed binding was due to the specific aptamers instead of nonspecific artifacts.

The response of Caff204 was similar to that of Caff203, except that the three analogs all showed slightly stronger binding. Therefore, it might have a larger contact area with caffeine. Caff209 had the highest selectivity for caffeine among these four aptamers, and we reason that the aptamer might interact with all the three methyl groups. Based on the patterns of binding, we deduced the orientation of binding. Caffeine has three exocyclic methyl groups, and the three analogs are generated by replacing each methyl group with a hydrogen. Regarding the methyl groups, we can consider that caffeine has a high 'symmetry'. If an aptamer's binding does not require a particular methyl group, demethylation of that methyl group might not affect binding. Based on this, we illustrated the orientation of binding on the right side of Figure 2. Here, we only emphasized the effect of the methyl groups, and other types of binding interactions such as π - π stacking are not shown. We did not find a sequence that can bind both caffeine and theophylline likely because we used theophylline as a counter target for the selection. Table S3 shows the binding

thermodynamic values, where the negative entropy change indicated that all the reactions were enthalpy driven.

Based on the different binding patterns obtained in Figure 2, it might be possible to use these four sequences collectively as a sensor array for discriminating all the analogs. This experiment also tells us that by using a target molecule with a high chemical symmetry, aptamers for binding to its symmetry-broken analogs might be obtained in the same selection.

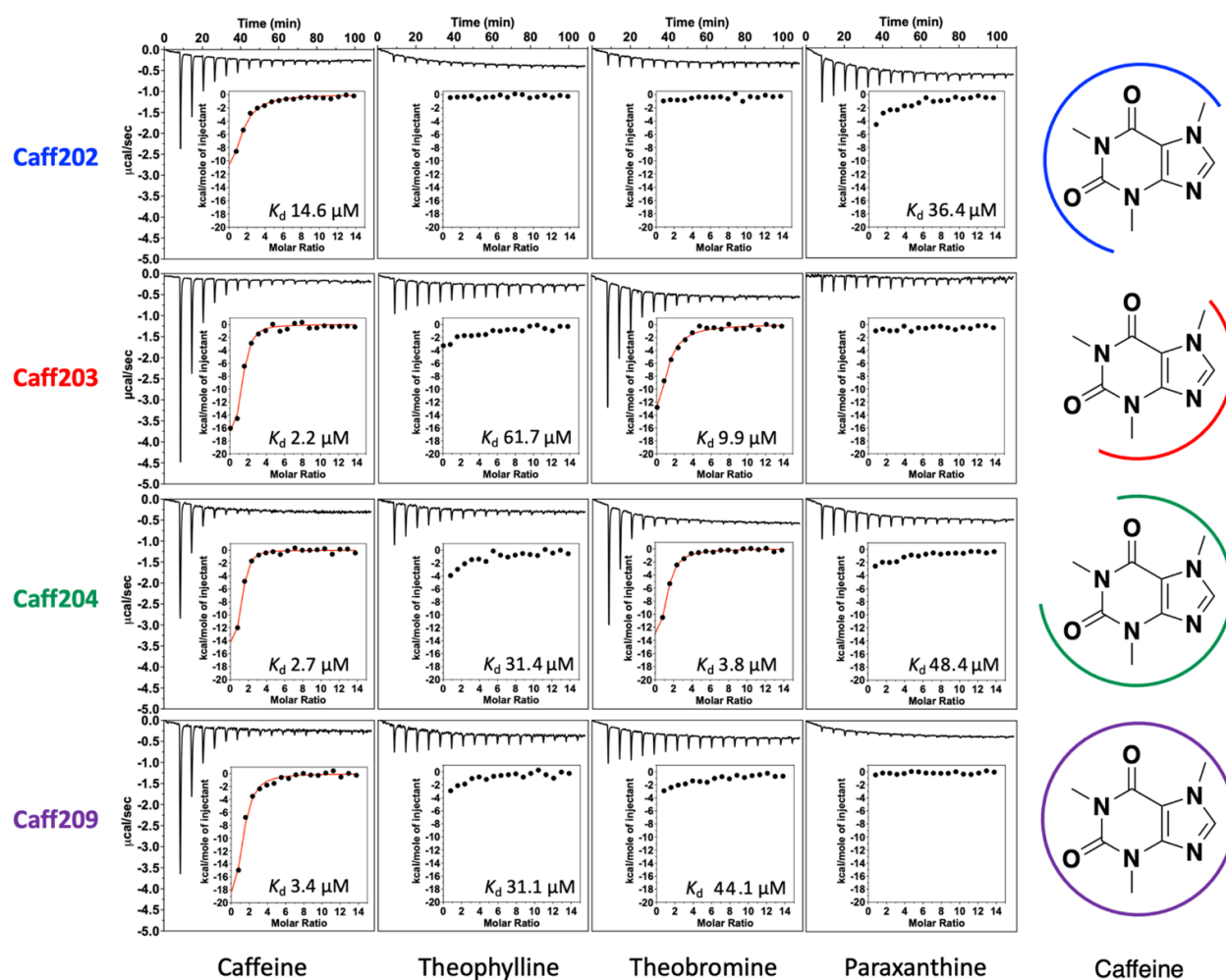


Figure 2. ITC analysis of the four caffeine-binding aptamers. For each titration, 1 mM of target was titrated into 9 μ M aptamer in the SELEX buffer at 25°C. Insets: the integrated heat and fitted K_d values. Right panels: schematic illustration showing the possible orientations of the aptamers binding to caffeine. Other interactions such as π - π stacking are not shown.

Fluorescent sensing of caffeine

Since the selection method was based on the structure-switching property of aptamers,^{34, 36, 39, 41} we took advantage of it to design biosensors. Out of the four aptamers, we decided to test Caff203 and Caff209 for sensing applications. Caff203 had the highest binding affinity for caffeine, while Caff209 had the best overall selectivity. The Caff203 data are discussed first (Figure 3A). The Caff203 aptamer sequence is shown in blue and it was extended by five nucleotides shown in red. A FAM fluorophore was labeled on the end. Then, a 12-mer DNA with a quencher was hybridized to mask the fluorescence. In the presence of caffeine, aptamer binding would result in the release of the quencher-labeled strand and fluorescence enhancement.

We used 20 nM of the FAM-labeled strand and 40 nM of the quencher-labeled strand to achieve a low background. When caffeine was added, the fluorescence immediately increased, while the sensor without caffeine added remained stable (Figure 3B). The higher the caffeine concentration, the stronger the final fluorescence. After 20 min of reaction, the fluorescence reached stable values for all the samples. With 1 mM caffeine, the fluorescence enhancement reached 9-fold. Based on the fluorescence increase at 20 min, a calibration curve with an apparent K_d of 80.5 μM was obtained (Figure 3C). This value was 37-fold highly than measured from ITC due to the competition from the short complementary DNA.³⁶ Below 100 μM caffeine, the response was linear (inset of Figure 3C). The detection limit was calculated to be 1.2 μM caffeine based on signal being greater than three times of background variation ($3\sigma/\text{slope}$).

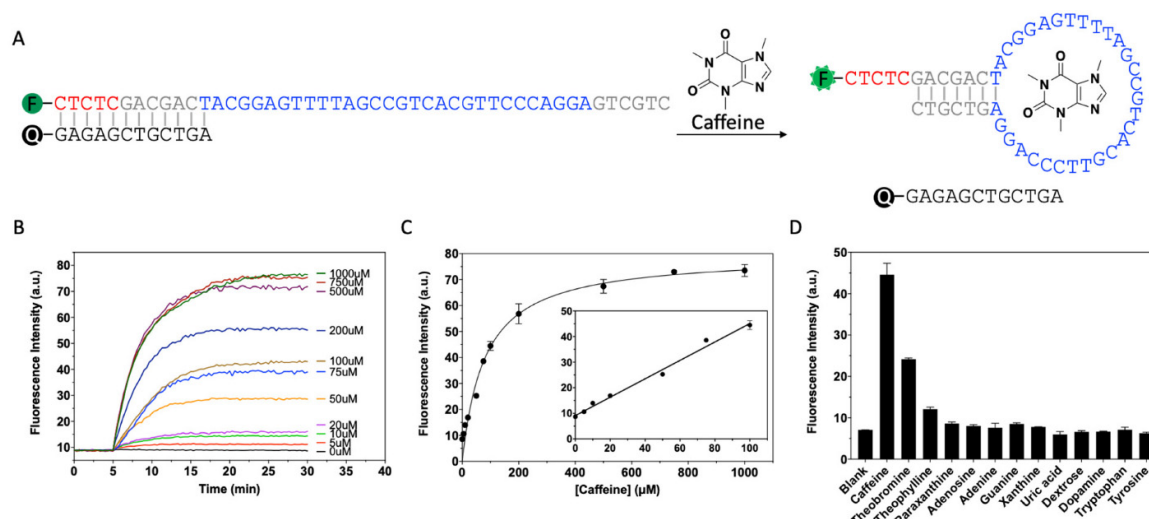


Figure 3. (A) Scheme of a fluorescent structure-switching signaling aptamer biosensor for the detection of caffeine. (B) Kinetics traces of 20 nM sensor in the presence of various concentrations of caffeine in the SELEX buffer. Noted that caffeine was added at the 5 min mark. (C) Fluorescence intensity as a

function of caffeine concentration. Inset: the linear response at low caffeine concentrations. (D) Sensor selectivity with 100 μM of various metabolites and purine analogues.

The sensitivity for Caff209 was also measured, and caffeine-dependent fluorescence enhancement was also achieved (Figure S6). Interestingly, the apparent K_d from the sensor (4.6 μM) was quite similar to that from ITC (3.4 μM). This result suggests that for the Caff209 sensor, the aptamer had a stronger tendency to fold back upon itself to close the hairpin and the quencher-labeled DNA was binding less tightly, explaining the high background. The saturated signal increase for the Caff209 sensor was only about 1.3-fold, while Caff203 had more than 7-fold increase. We chose Caff203 for the subsequent sensor tests, since it had the highest caffeine binding affinity and much lower background.

For selectivity test, 100 μM caffeine or its analogs were added to the Caff203 sensor and the data are presented in Figure 3D. Theobromine showed the next highest signal, and the other biomolecules were mostly in the background level, consistent with the ITC-based results. In particular, no response was seen for adenosine. Since caffeine is an antagonist of adenosine,⁵⁴ this selectivity might be useful for neuroscience.

Analysis of caffeine in beverages

To understand the performance of the sensor for real sample analysis, a few caffeine-containing drinks like coffee, tea and soda were tested (Figure 4). Caffeine pills were also tested by dissolving them in Milli-Q water to achieve a stock concentration of 1 mg/mL. For each test, 2 μL of sample was added to 100 μL of 20 nM sensor (51-fold dilution) for 30 min before measurement. Among all the samples, the Starbucks doubleshot coffee had a higher background due to the milk in the coffee. Nevertheless, the enhancement of fluorescence due to the sensor response could still be recorded. The estimated concentration was then extrapolated from the standard curve. The concentration detected by the sensor corresponded closely within 6.1% difference compared to the caffeine contents indicated on the labels (Figure 4). Previous studies have showed that the labeled caffeine contents from such drinks were within 10% to 15% difference compared to the values measured by instrumentation methods.^{55, 56} Therefore, we compared our sensor results with the labeled caffeine content.

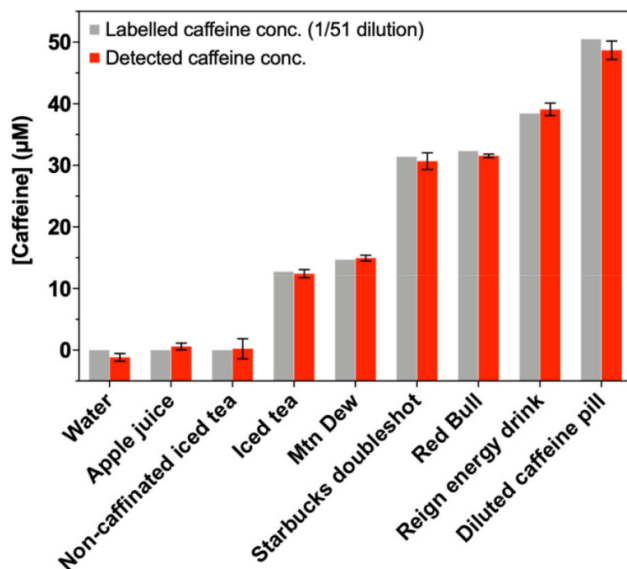


Figure 4. Sensor performance with various off the shelf beverages.

Based on an HPLC study of over twenty types of commercial coffees and teas, none of the coffees contained any theobromine, while the theobromine content was typically below 6% compared of the caffeine content in the non-decaffeinated teas.⁵⁷ In coffees, the content of theophylline is typically below 0.03% of that of caffeine, while the level of paraxanthine is even less.⁵⁸ Given the selectivity of this sensor, the interference from theobromine in these samples would be less than 3%, and the interference from the other two analogs was negligible. Therefore, this simple sensor was able to achieve a high accuracy in real samples. For some drinks, such as hot coco mix, the theobromine concentration was higher than caffeine.⁵⁷ For those samples, a single sensor does not have sufficient selectivity. Fortunately, we have four different sensors, which may collectively improve selectivity as shown in the next section.

Aside from testing the sensor in beverages, we also tested human blood serum. In a recent study, the average serum caffeine concentration was 2.7 μM before drinking coffee, which increased to 20.7 μM after drinking.⁵⁹ Due to the strong light scattering of serum and increased background, we diluted it with the SELEX buffer to 20% serum for the experiment. A caffeine concentration dependent fluorescence enhancement was also observed, and the limit of detection was calculated to be 4.0 μM (Figure S7A, B). The selectivity pattern was also comparable to that in buffer (Figure S7C). We have also compared the performance of our sensor with other fluorescent caffeine biosensors reported in the literature, and our study was the most comprehensive and had the best performance combining sensitivity and selectivity (Table S4).

Discrimination of the single demethylated analogs using a sensor array

With the four aptamer sensors, we then tested their specificity to a total of 13 closely related biomolecules (Figure 5A). The distinct response patterns allowed us to form a sensor array containing the four sensors. By using principal component analysis (PCA), we could identify the analytes especially the four methylxanthine easily.^{60, 61} PCA is a useful tool for multivariate statistical analysis. This technique helps reducing the dimensionality of a large datasets, increasing interpretability while minimizing information loss during the process. The PCA plot shows clusters of samples based on their similarity. In this case, thirteen biomolecules were grouped into seven clusters (Figure 5B). Importantly, caffeine and its analogs are well separated.

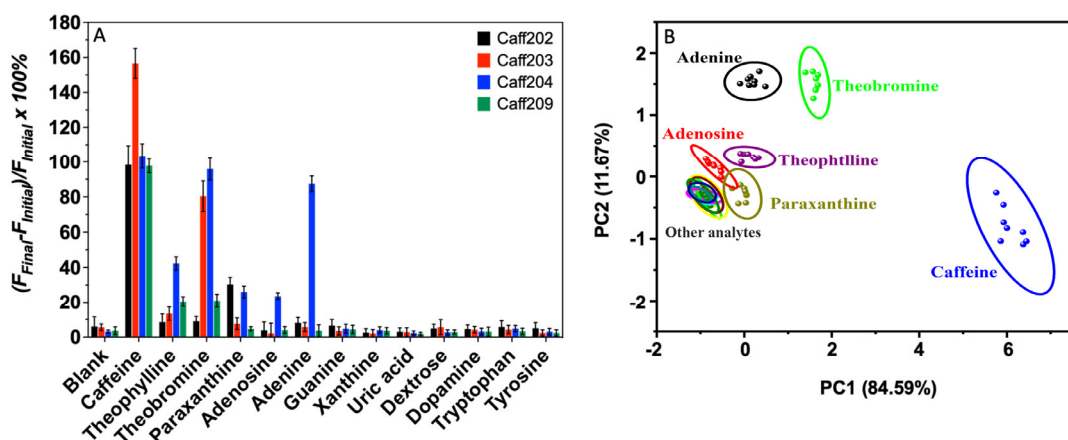


Figure 5. (A) Percentage of fluorescence enhancement of four aptamer sensors in the presence of 20 μ M different biomolecules after 20 min incubation. (B) PCA scores of 13 analytes from four different caffeine aptamer sensors. The data showed clusters of seven with caffeine far off from other analytes. The data was generated with eight sets of repetitions. The ellipses indicate regions with a 95% confidence level.

Conclusions

In conclusion, we selected four high-quality DNA aptamers for caffeine with excellent binding affinity and specificity. The selection results indicated the importance of molecular symmetry in the evolution of aptamers. With the three methyl group in caffeine, different aptamers were obtained to bind different parts of the target, and removing a non-binding methyl group would not affect the binding much. A fluorescent biosensor for caffeine was designed and a detection of limit of 1.2 μM caffeine was obtained. A total of eight caffeine containing drinks were tested and the sensor could accurately measure the caffeine concentrations. Some aptamers could also bind single demethylated analogs, allowing the detection of all of them using a sensor array containing the four aptamer sensors. Given the importance of caffeine in daily life, biology and environmental chemistry, we expect these aptamers to be used as another important model system for developing biosensors.

Acknowledgements

Funding for this work was from the Global Water Future project of the Canada First Research Excellence Fund (CFREF), and the Natural Sciences and Engineering Research Council of Canada (NSERC).

Supporting Information Available

Aptamer selection scheme, conditions, and progress analyzed by real-time PCR, aptamer sequence alignment, additional ITC traces with other analytes and mutated non-binding aptamers. Sensing data based on Caff209, and sensing in serum, and DNA sequences, and a table to compare our caffeine sensor with the previously published ones.

References

- (1) Temple, J. L.; Bernard, C.; Lipshultz, S. E.; Czachor, J. D.; Westphal, J. A.; Mestre, M. A., The Safety of Ingested Caffeine: A Comprehensive Review. *Front. Psychiatry* **2017**, *8*.

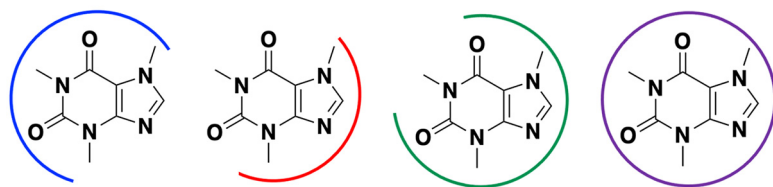
-
- (2) Korekar, G.; Kumar, A.; Ugale, C., Occurrence, Fate, Persistence and Remediation of Caffeine: A Review. *Environ. Sci. Pollut. Res.* **2020**, *27*, 34715-34733.
 - (3) Spence, P. L., Using Caffeine as a Water Quality Indicator in the Ambient Monitoring Program for Third Fork Creek Watershed, Durham, North Carolina. *Environ. Health Insights* **2020**, *9*, 29-34.
 - (4) Lopez-Sanchez, R. D.; Lara-Diaz, V. J.; Aranda-Gutierrez, A.; Martinez-Cardona, J. A.; Hernandez, J. A., Hplc Method for Quantification of Caffeine and Its Three Major Metabolites in Human Plasma Using Fetal Bovine Serum Matrix to Evaluate Prenatal Drug Exposure. *J. Anal. Meth. Chem.* **2018**, *2018*, 2085059.
 - (5) Xu, W.; Kim, T.-H.; Zhai, D.; Er, J. C.; Zhang, L.; Kale, A. A.; Agrawalla, B. K.; Cho, Y.-K.; Chang, Y.-T., Make Caffeine Visible: A Fluorescent Caffeine “Traffic Light” Detector. *Sci. Rep.* **2013**, *3*, 2255.
 - (6) Smith, J.; Loxley, K.; Sheridan, P.; Hamilton, T. M., Analysis of Caffeine in Beverages: Using Aspirin as a Fluorescent Chemosensor. *J. Chem. Educ.* **2016**, *93*, 1776-1780.
 - (7) Dey, N.; Maji, B.; Bhattacharya, S., A Versatile Probe for Caffeine Detection in Real-Life Samples Via Excitation-Triggered Alteration in the Sensing Behavior of Fluorescent Organic Nanoaggregates. *Anal. Chem.* **2018**, *90*, 821-829.
 - (8) Karmakar, P.; Manna, S.; Maiti, K.; Ali, S. S.; Guria, U. N.; Sarkar, R.; Datta, P.; Mandal, D.; Mahapatra, A. K., A Perylene Diimide Based Fluorescent Probe for Caffeine in Aqueous Medium. *Supramol. Chem.* **2019**, *31*, 28-35.
 - (9) Du, C. X.; Ma, C. Q.; Gu, J.; Li, L.; Chen, G. Q., Fluorescence Sensing of Caffeine in Tea Beverages with 3,5-Diaminobenzoic Acid. *Sensors* **2020**, *20*, 819.
 - (10) Oberleitner, L.; Grandke, J.; Mallwitz, F.; Resch-Genger, U.; Garbe, L.-A.; Schneider, R. J., Fluorescence Polarization Immunoassays for the Quantification of Caffeine in Beverages. *J. Agric. Food. Chem.* **2014**, *62*, 2337-2343.
 - (11) Khoo, W. Y. H.; Pumera, M.; Bonanni, A., Graphene Platforms for the Detection of Caffeine in Real Samples. *Anal. Chim. Acta* **2013**, *804*, 92-97.
 - (12) Betlem, K.; Mahmood, I.; Seixas, R. D.; Sadiki, I.; Raimbault, R. L. D.; Foster, C. W.; Crapnell, R. D.; Tedesco, S.; Banks, C. E.; Gruber, J.; Peeters, M., Evaluating the Temperature Dependence of Heat-Transfer Based Detection: A Case Study with Caffeine and Molecularly Imprinted Polymers as Synthetic Receptors. *Chem. Eng. J.* **2019**, *359*, 505-517.
 - (13) Rankin, C. J.; Fuller, E. N.; Hamor, K. H.; Gabarra, S. A.; Shields, T. P., A Simple Fluorescent Biosensor for Theophylline Based on Its RNA Aptamer. *Nucleos. Nucleot. Nucl.* **2006**, *25*, 1407-1424.
 - (14) Martínez-Pinilla, E.; Oñatibia-Astibia, A.; Franco, R., The Relevance of Theobromine for the Beneficial Effects of Cocoa Consumption. *Front. Pharmacol.* **2015**, *6*, 30.
 - (15) Orrú, M.; Guitart, X.; Karcz-Kubicha, M.; Solinas, M.; Justinova, Z.; Barodia, S. K.; Zanoveli, J.; Cortes, A.; Lluís, C.; Casado, V.; Moeller, F. G.; Ferré, S., Psychostimulant Pharmacological Profile of Paraxanthine, the Main Metabolite of Caffeine in Humans. *Neuropharmacology* **2013**, *67*, 476-484.
 - (16) Li, L.; Xu, S. J.; Yan, H.; Li, X. W.; Yazd, H. S.; Li, X.; Huang, T.; Cui, C.; Jiang, J. H.; Tan, W. H., Nucleic Acid Aptamers for Molecular Diagnostics and Therapeutics: Advances and Perspectives. *Angew. Chem. Int. Ed.* **2021**, *60*, 2221-2231.
 - (17) Dunn, M. R.; Jimenez, R. M.; Chaput, J. C., Analysis of Aptamer Discovery and Technology. *Nat. Rev. Chem.* **2017**, *1*, 0076.

-
- (18) Wu, Y.; Belmonte, I.; Sykes, K. S.; Xiao, Y.; White, R. J., Perspective on the Future Role of Aptamers in Analytical Chemistry. *Anal. Chem.* **2019**, 91, 15335-15344.
- (19) Wang, J.; Yu, J.; Yang, Q.; McDermott, J.; Scott, A.; Vukovich, M.; Lagrois, R.; Gong, Q.; Greenleaf, W.; Eisenstein, M.; Ferguson, B. S.; Soh, H. T., Multiparameter Particle Display (MPPD): A Quantitative Screening Method for the Discovery of Highly Specific Aptamers. *Angew. Chem. Int. Ed.* **2017**, 56, 744-747.
- (20) Yu, H.; Alkhamis, O.; Canoura, J.; Liu, Y.; Xiao, Y., Advances and Challenges in Small-Molecule DNA Aptamer Isolation, Characterization, and Sensor Development. *Angew. Chem. Int. Ed.* **2021**, 60, 16800-16823.
- (21) Alkhamis, O.; Canoura, J.; Yu, H. X.; Liu, Y. Z.; Xiao, Y., Innovative Engineering and Sensing Strategies for Aptamer-Based Small-Molecule Detection. *TrAC, Trends Anal. Chem.* **2019**, 121, 115699.
- (22) Ruscito, A.; DeRosa, M. C., Small-Molecule Binding Aptamers: Selection Strategies, Characterization, and Applications. *Front. Chem.* **2016**, 4, 14.
- (23) Roth, A.; Breaker, R. R., The Structural and Functional Diversity of Metabolite-Binding Riboswitches. *Annu. Rev. Biochem.* **2009**, 78, 305-334.
- (24) Tuerk, C.; Gold, L., Systematic Evolution of Ligands by Exponential Enrichment: RNA Ligands to Bacteriophage T4 DNA Polymerase. *Science* **1990**, 249, 505-510.
- (25) Ellington, A. D.; Szostak, J. W., In Vitro Selection of RNA Molecules That Bind Specific Ligands. *Nature* **1990**, 346, 818-822.
- (26) Pang, X. H.; Cui, C.; Wan, S.; Jiang, Y.; Zhang, L. L.; Xia, L.; Li, L.; Li, X. W.; Tan, W. H., Bioapplications of Cell-SeleX-Generated Aptamers in Cancer Diagnostics, Therapeutics, Theranostics and Biomarker Discovery: A Comprehensive Review. *Cancers* **2018**, 10.
- (27) Liu, M.; Yin, Q.; Chang, Y.; Zhang, Q.; Brennan, J. D.; Li, Y., In Vitro Selection of Circular DNA Aptamers for Biosensing Applications. *Angew. Chem. Int. Ed.* **2019**, 58, 8013-8017.
- (28) Hamula, C. L. A.; Zhang, H.; Li, F.; Wang, Z.; Chris Le, X.; Li, X.-F., Selection and Analytical Applications of Aptamers Binding Microbial Pathogens. *TrAC, Trends Anal. Chem.* **2011**, 30, 1587-1597.
- (29) Xing, H.; Wong, N. Y.; Xiang, Y.; Lu, Y., DNA Aptamer Functionalized Nanomaterials for Intracellular Analysis, Cancer Cell Imaging and Drug Delivery. *Curr. Opin. Chem. Biol.* **2012**, 16, 429-435.
- (30) Yu, H.; Luo, Y.; Alkhamis, O.; Canoura, J.; Yu, B.; Xiao, Y., Isolation of Natural DNA Aptamers for Challenging Small-Molecule Targets, Cannabinoids. *Anal. Chem.* **2021**, 93, 3172-3180.
- (31) Shkempi, X.; Skouridou, V.; Svobodova, M.; Leonardo, S.; Bashammakh, A. S.; Alyoubi, A. O.; Campàs, M.; O'Sullivan, C. K., Hybrid Antibody-Aptamer Assay for Detection of Tetrodotoxin in Pufferfish. *Anal. Chem.* **2021**, 93, 14810-14819.
- (32) Jenison, R. D.; Gill, S. C.; Pardi, A.; Polisky, B., High-Resolution Molecular Discrimination by RNA. *Science* **1994**, 263, 1425-1429.
- (33) Wrist, A.; Sun, W.; Summers, R. M., The Theophylline Aptamer: 25 Years as an Important Tool in Cellular Engineering Research. *ACS Synth. Biol.* **2020**, 9, 682-697.
- (34) Nakatsuka, N.; Yang, K.-A.; Abendroth, J. M.; Cheung, K. M.; Xu, X.; Yang, H.; Zhao, C.; Zhu, B.; Rim, Y. S.; Yang, Y.; Weiss, P. S.; Stojanović, M. N.; Andrews, A. M., Aptamer-Field-Effect Transistors Overcome Debye Length Limitations for Small-Molecule Sensing. *Science* **2018**, 362, 319-324.

-
- (35) Yang, K.-A.; Pei, R.; Stojanovic, M. N., In Vitro Selection and Amplification Protocols for Isolation of Aptameric Sensors for Small Molecules. *Methods* **2016**, 106, 58-65.
- (36) Nutiu, R.; Li, Y., Structure-Switching Signaling Aptamers. *J. Am. Chem. Soc.* **2003**, 125, 4771-4778.
- (37) Feagin, T. A.; Maganzini, N.; Soh, H. T., Strategies for Creating Structure-Switching Aptamers. *ACS Sensors* **2018**, 3, 1611-1615.
- (38) Yang, K.-A.; Pei, R.; Stefanovic, D.; Stojanovic, M. N., Optimizing Cross-Reactivity with Evolutionary Search for Sensors. *J. Am. Chem. Soc.* **2012**, 134, 1642-1647.
- (39) Nutiu, R.; Li, Y., In Vitro Selection of Structure-Switching Signaling Aptamers. *Angew. Chem. Int. Ed.* **2005**, 44, 1061-1065.
- (40) Rajendran, M.; Ellington, A. D., Selection of Fluorescent Aptamer Beacons That Light up in the Presence of Zinc. *Anal. Bioanal. Chem.* **2008**, 390, 1067-1075.
- (41) Yang, W. J.; Yu, H. X.; Alkhamis, O.; Liu, Y. Z.; Canoura, J.; Fu, F. F.; Xiao, Y., In Vitro Isolation of Class-Specific Oligonucleotide-Based Small-Molecule Receptors. *Nucleic Acids Res.* **2019**, 47, e71.
- (42) Yu, H. X.; Yang, W. J.; Alkhamis, O.; Canoura, J.; Yang, K. A.; Xiao, Y., In Vitro Isolation of Small-Molecule-Binding Aptamers with Intrinsic Dye-Displacement Functionality. *Nucleic Acids Res.* **2018**, 46, e43.
- (43) Qu, H.; Csordas, A. T.; Wang, J.; Oh, S. S.; Eisenstein, M. S.; Soh, H. T., Rapid and Label-Free Strategy to Isolate Aptamers for Metal Ions. *ACS Nano* **2016**, 10, 7558-7565.
- (44) Zhang, A. Z.; Chang, D. R.; Zhang, Z. J.; Li, F.; Li, W. H.; Wang, X.; Li, Y. F.; Hua, Q., In Vitro Selection of DNA Aptamers That Binds Geniposide. *Molecules* **2017**, 22.
- (45) Gu, C.; Lan, T.; Shi, H.; Lu, Y., Portable Detection of Melamine in Milk Using a Personal Glucose Meter Based on an in Vitro Selected Structure-Switching Aptamer. *Anal. Chem.* **2015**, 87, 7676-7682.
- (46) Luo, Y.; Wang, J.; Yang, L.; Gao, T.; Pei, R., In Vitro Selection of DNA Aptamers for the Development of Fluorescent Aptasensor for Sarcosine Detection. *Sens. Actuators B Chem.* **2018**, 276, 128-135.
- (47) Zuker, M., Mfold Web Server for Nucleic Acid Folding and Hybridization Prediction. *Nucleic Acids Res.* **2003**, 31, 3406-3415.
- (48) Slavkovic, S.; Johnson, P. E., Isothermal Titration Calorimetry Studies of Aptamer-Small Molecule Interactions: Practicalities and Pitfalls. *Aptamers* **2018**, 2, 45-51.
- (49) Neves, M. A. D.; Slavkovic, S.; Churcher, Z. R.; Johnson, P. E., Salt-Mediated Two-Site Ligand Binding by the Cocaine-Binding Aptamer. *Nucleic Acids Res.* **2016**, 45, 1041-1048.
- (50) Oni, O.; Zhang, Z.; Liu, J., New Insights into a Classic Aptamer: Binding Sites, Cooperativity and More Sensitive Adenosine Detection. *Nucleic Acids Res.* **2017**, 45, 7593-7601.
- (51) Ferapontova, E. E.; Olsen, E. M.; Gothelf, K. V., An RNA Aptamer-Based Electrochemical Biosensor for Detection of Theophylline in Serum. *J. Am. Chem. Soc.* **2008**, 130, 4256-4258.
- (52) Wiseman, T.; Williston, S.; Brandts, J. F.; Lin, L.-N., Rapid Measurement of Binding Constants and Heats of Binding Using a New Titration Calorimeter. *Anal. Biochem.* **1989**, 179, 131-137.
- (53) Turnbull, W. B.; Daranas, A. H., On the Value of C: Can Low Affinity Systems Be Studied by Isothermal Titration Calorimetry? *J. Am. Chem. Soc.* **2003**, 125, 14859-14866.
- (54) López-Cruz, L.; Salamone, J. D.; Correa, M., Caffeine and Selective Adenosine Receptor Antagonists as New Therapeutic Tools for the Motivational Symptoms of Depression. *Front. Pharmacol.* **2018**, 9, 526.

-
- (55) Al-Bratty, M.; Alhazmi, H. A.; Rehman, Z. u.; Javed, S. A.; Ahsan, W.; Najmi, A.; Khuwaja, G.; Makeen, H. A.; Khalid, A., Determination of Caffeine Content in Commercial Energy Beverages Available in Saudi Arabian Market by Gas Chromatography-Mass Spectrometric Analysis. *J. Spectrosc.* **2020**, 2020, 3716343.
- (56) Attipoe, S.; Leggit, J.; Deuster, P. A., Caffeine Content in Popular Energy Drinks and Energy Shots. *Mil. Med.* **2016**, 181, 1016-1020.
- (57) BLAUCH, J. L.; TARKA JR., S. M., Hplc Determination of Caffeine and Theobromine in Coffee, Tea, and Instant Hot Cocoa Mixes. *J. Food Sci.* **1983**, 48, 745-747.
- (58) Spiller, M. A., The Chemical Components of Coffee. In *The Methylxanthine Beverages and Foods: Chemistry, Consumption, and Health Effects*, Spiller, G. A., Ed. Alan R. Liss: New York, 1984; pp 91–147.
- (59) Ohmichi, T.; Kasai, T.; Shinomoto, M.; Matsuura, J.; Koizumi, T.; Kitani-Morii, F.; Tatebe, H.; Sasaki, H.; Mizuno, T.; Tokuda, T., Quantification of Blood Caffeine Levels in Patients with Parkinson's Disease and Multiple System Atrophy by Caffeine Elisa. *Front. Neurol.* **2020**, 11, 580127.
- (60) Chen, Z. H.; Fan, Q. X.; Han, X. Y.; Shi, G. Y.; Zhang, M., Design of Smart Chemical 'Tongue' Sensor Arrays for Pattern-Recognition-Based Biochemical Sensing Applications. *TrAC Trends Anal. Chem.* **2020**, 124.
- (61) Geng, Y.; Peveler, W. J.; Rotello, V. M., Array-Based "Chemical Nose" Sensing in Diagnostics and Drug Discovery. *Angew. Chem. Int. Ed.* **2019**, 58, 5190-5200.

For Table of Content Graphics Only



Possible orientations of caffeine binding by its four aptamers